# Fast $C_Z$ gate for ultracold neutral atoms based on counterdiabatic driving at Rydberg excitation

### I. I. Beterov

Rzhanov Institute of Semiconductor Physics SB RAS, 630090 Novosibirsk, Russia Novosibirsk State University, 630090 Novosibirsk, Russia Novosibirsk State Technical University, 630073 Novosibirsk, Russia and Institute of Laser Physics SB RAS, 630090 Novosibirsk, Russia

#### K.V. Kozenko and I.I. Ryabtsev ©

Rzhanov Institute of Semiconductor Physics SB RAS, 630090 Novosibirsk, Russia and Novosibirsk State University, 630090 Novosibirsk, Russia

### Peng Xu 💿

State Key Laboratory of Magnetic Resonance and Atomic and Molecular Physics, Innovation Academy for Precision Measurement Science and Technology, Chinese Academy of Sciences, Wuhan 430071, China and Wuhan Institute of Quantum Technology, Wuhan 430206, China (Dated: November 13, 2025)

We designed the scheme of neutral atom Rydberg blockade  $C_Z$  gate based on double sequence of adiabatic pulses applied symmetrically to both atoms using counterdiabatic driving at Rydberg excitation. This provides substantial reducing of quantum gate operation time compared to previously proposed double adiabatic schemes, and makes this scheme competitive with modern time-optimal protocols for high-fidelity entangling gates with neutral atoms. Our approach creates the bridge between fully adiabatic and time-optimal gate schemes. The use of adiabatic passage reduces the sensitivity of gate fidelity on variation of laser intensity, and counterdiabatic driving provides short gate times. The intensity and phase profile of the laser pulse acting on atoms is described analytically depending on the gate duration only. We show that the upper limit of the Bell fidelity reaches  $\mathcal{F} \simeq 0.9999$  in a room-temperature environment for realistic values of Rydberg lifetimes and Rydberg blockade strength. We demonstrated the applicability of this scheme for single-photon, two-photon and three-photon configurations of Rydberg excitation for rubidium and cesium atoms.

#### I. INTRODUCTION

Quantum computing with ultracold neutral atoms has greatly advanced in the recent years. Large-scale atomic arrays containing thousands of qubits have been demonstrated [1, 2] and quantum algorithms were successfully implemented [3–5]. There are new promising architectures for neutral-atom quantum computing based on logical qubits [6] and new technological approaches, for example, using fiber arrays [7]. The fidelity of two-qubit gates in the experiment reached 99.7% [8], opening the way to quantum error correction and design of the logical qubits [6, 9]. High-fidelity entanglement with neutral atoms is achieved using Rydberg blockade [10] and carefully designed amplitude and phase profiles of laser pulses, which are used for Rydberg excitation [8, 11–13]. The parameters of these pulses are usually obtained using numeric optimization of the gate performance [8, 12–14]. Optimal control theory is also used for preparation of the desired quantum states [15], and in particular for design of high-fidelity gates [16]. There are also alternative gate schemes which do not rely on Rydberg blockade [17, 18].

An important feature of modern high-fidelity gate protocols for neutral atoms is that they are always symmetric, as both interacting atoms are illuminated by identical laser pulses [8, 11]. At the same time, the dynamics of

a two-atom system depends on its initial state and the energy of interatomic interaction, which results in the entanglement between the atoms. Symmetric driving by identical laser pulses has numerous advantages, including the ability to implement quantum gates in a parallel way [13] in large atomic arrays, and higher entanglement fidelity, which is achieved due to short time duration of single Rydberg excitation and the reduced spatial inhomogeneity of wide laser beams, which excite the atoms into Rydberg states [8, 11, 13].

In the experiment, high-fidelity entanglement of two neutral atoms was demonstrated using Levine-Pichler gate [11] and time-optimal protocols [8, 12–14]. Recently, Fromonteil et al. designed an interesting 5-pulse sequence following the refocusing technique in NMR [19]. This work emphasizes remaining interest in purely analytical approaches for implementation of high-fidelity entangling gates, when there is no need to parametrize the complex profiles of laser pulses using numbers obtained from extensive numeric optimization.

In our previous works we proposed a double-pulse adiabatic sequence which provides a  $\pi$  phase shift of the two-level system when it returns to the initial state after excitation and de-excitation [20, 21]. This phase shift results from phase accumulation during adiabatic passage and can be understood from simple analytical for-

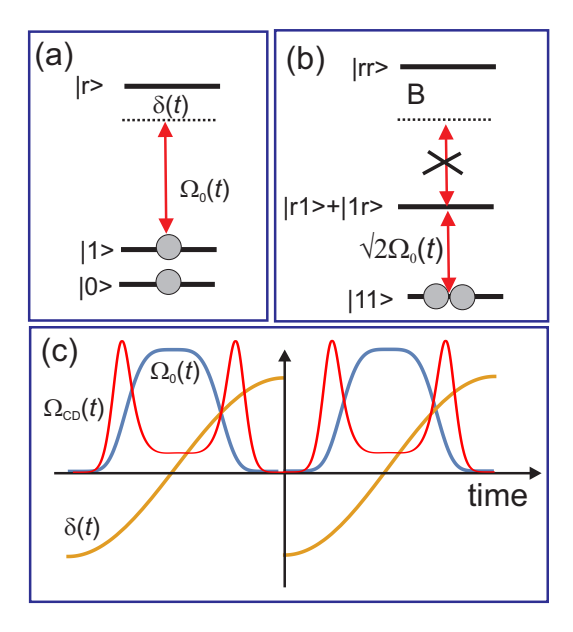


FIG. 1. (color online) (a) Energy level structure of atom qubit with logical states represented by ground state sublevels  $|0\rangle, |1\rangle$  and Rydberg state  $|r\rangle$  coupled to state  $|1\rangle$  by resonant laser radiation with Rabi frequency  $\Omega_0(t)$  and detuning  $\delta(t)$ . (b) Rydberg atoms in state  $|r\rangle$  interact with strength B which results in Rydberg blockade. When two nearby atoms in ground state |1| are illuminated by resonant laser radiation, only one atom is excited to Rydberg state. The two-atom system is effectively a two-level system with states  $|11\rangle$  and  $\frac{1}{\sqrt{2}}(|r1\rangle + |1r\rangle)$  with enhanced coupling  $\sqrt{2}\Omega_0(t)$  between them. (c) Double adiabatic sequence results in accumulation of  $\pi$  phase shift after excitation and de-excitation of two-atom system prepared initially in each of the states  $|01\rangle$ ,  $|10\rangle$ ,  $|11\rangle$ . The state  $|00\rangle$  remains unaffected. The phase-shifted pulse  $\Omega_{\rm CD}$  (t) represents a counterdiabatic term which is necessary to speed-up the gate.

mulas [20]. The proposal for symmetric quantum gates based on double adiabatic sequence [21] attracted substantial interest in the recent years [3, 13, 14, 16, 22–66]. Recently, it has been shown that such double-pulse adiabatic sequence can be used for entangling distant qubits in the atomic ensemble [55]. The main advantage of the adiabatic passage is the reduced sensitivity of gate fidelity on the variations of intensity of laser radiation.

However, the double adiabatic passage has not yet been successfully used for experimental implementation of high-fidelity two-qubit gates. One of the possible reasons is that the adiabatic protocols are intrinsically slow, which is a great disadvantage due to finite lifetimes of Rydberg atomic states [67] and finite Rydberg blockade strengths, which limit the possibility to speed-up the gate merely by increased Rabi frequency. Therefore it is important to design the schemes of quantum gates combining short gate time and moderate values of the driving Rabi frequency. The shortcut to adiabaticity [68–75] is a well-known approach which allows for implementation of fast adiabatic excitation schemes by suppression

of the nonadiabatic transition to the undesired states. In the counterdiabatic driving the additional term is directly included in the Hamiltonian in order to eliminate the nonadiabatic coupling. This term is a function of time-dependent Rabi frequency and the detuning from the resonance in a two-level system. Counterdiabatic driving also attracts a lot of interest in modern quantum information processing [39, 76–79]. It has been proposed to use contridabatic driving to suppress noise in CNOT gates [80]. Recently, preparation of Rydberg superatoms using counterdiabatic driving was studied [81]. A  $C_Z$  gate for superconducting qubits using shortcut to adiabaticity was demonstrated experimentally [82].

Although it seems to be straightforward to use shortcut to adiabaticity to speed-up two-qubit gates based on adiabatic rapid passage, the research in this area is limited. Acceleration of the double adiabatic passage for  $C_Z$  gate using shortcut to adiabaticity was first proposed in Ref. [54]. However, the authors of that work found that in the regime of Rydberg blockade due to  $\sqrt{2}$  enhancement of the Rabi frequency [11, 83, 84], the conditions of counterdiabatic driving cannot be met simultaneously for one atom and for two interacting atoms. They did not solve this problem completely, since they used a non-separable driving Hamiltonian for the system of two atoms.

The second work which addressed this task is Ref. [66]. The authors proposed a more complex four-pulse protocol which allowed shortening of the gate twice to  $0.24\,\mu\text{s}$ , compared to the initial double-pulse scheme from Ref. [21]. However, due to finite Rydberg lifetimes shorter and fully scalable time-optimal protocols are more promising [8].

In this paper we show that for two-pulse adiabatic pulse sequence it is also possible to find the conditions to obtain the population and phase dynamics of the two-atom system, which is required for a  $C_Z$  gate operation. This allows substantial shortening of the gate time compared to the original proposal [21]. The overall performance of our gate is comparable to modern time-optical protocols [8, 11, 13, 14]. At the same time, because of the use of adiabatic passage, our gate scheme provides reduced sensitivity to variation of laser intensities.

The paper is organized as follows. In Sec. II we discuss the theory of counterdiabatic driving and present results of calculations for the ideal case of single-photon Rabi excitation without spontaneous decay and infinite blockade strength. We show that in this case the fidelity of entanglement can be close to one. In Sec. III we calculate the fidelity of entanglement for the simplest case of single-photon Rydberg excitation of rubidium and cesium atoms, taking into account spontaneous decay of Rydberg states. In Sec. IV we consider adiabatic rapid passage for the most common two-photon schemes of Rydberg excitation. In Sec.V we show that adiabatic rapid passage at three-photon laser excitation is also feasible for realistic experimental conditions and compare its performance with Levine-Pichler gate from [11] and time-optimal gate from [13], first time adopted for threephoton laser excitation. The results are summarized in Sec. VI.

### II. COUNTERDIABATIC DRIVING AND RYDBERG BLOCKADE

In the experiments on quantum computing with ultracold neutral atoms well isolated hyperfine sublevels of the ground state of alkali-metal atoms (usually rubidium and cesium) are used as qubit logical states  $|0\rangle$  and |1\), as shown in Fig. 1(a) [85]. When the atom is excited to the Rydberg state  $|r\rangle$  and returns back to the ground state, it accumulates a phase shift  $\pi$  which can be used for the  $C_Z$  gate [10, 86]. In the regime of Rydberg blockade, which is illustrated in Fig. 1(b), two atoms are simultaneously illuminated by laser radiation, which is tuned to the resonance with the transition into Rydberg state. Due to pairwise Rydberg interactions the collective energy state  $|rr\rangle$  obtains large energy shift B which is known as blockade strength [10]. Simultaneous laser excitation of two nearby Rydberg atoms becomes impossible, and the system of two interacting atoms is efficiently a two-level system with frequency of Rabi oscillations enhanced by a factor of  $\sqrt{2}$  compared to the single-photon Rabi frequency  $\Omega_0$  [83].

The scheme of double adiabatic sequence is shown in Fig. 1(c) [20]. During this sequence the atoms are excited from initial state  $|1\rangle$  to Rydberg state  $|r\rangle$ . Only one atom in a two-atom system can be excited due to Rydberg blockade. The second pulse returns the atoms to the initial state, and the phase shift  $\pi$  is accumulated by the whole two-atom system. This is equivalent to the entangling  $C_Z$  gate with an additional single-qubit phase shift. The counterdiabatic driving is provided by an additional field which can be obtained by modifying the time and phase profile of the driving laser pulse.

The  $\sqrt{2}$  enhancement of the Rabi frequency in the regime of Rydberg blockade results in the inability to simultaneously return the population to the ground state for such different initial states as  $|10\rangle$  and  $|11\rangle$ , using a single laser pulse with the same area. This can be overcome by using complex pulse shapes with numerically optimized amplitude and phase profiles [11, 14]. An alternative is adiabatic passage at Rydberg excitation [21]. Adiabatic rapid passage is common for laser excitation of molecular levels because of the independence of transition probability on the Rabi frequency [87, 88]. A number of schemes for quantum logic gates using two-photon stimulated Raman adiabatic passage (STIRAP) [89, 90] and Rydberg excitation have been developed [91, 92].

In our previous works [93, 94] we have found that double adiabatic rapid passage returns the system to the initial state, but with a phase shift. This shift is equal to  $\pi$  for two identical laser pulses and to zero if the second laser pulse is phase shifted by  $\pi$  [20]. This allowed us to develop schemes of quantum gates with mesoscopic atomic ensembles, using adiabatic passage and Rydberg

blockade [93, 94]. In particular, we designed a scheme of symmetric  $C_Z$  gate for two atoms [21]. Now we revise this scheme of adiabatic passage in order to introduce shortcut to adiabaticity [68, 95], following the idea from the previous proposal for acceleration of double adiabatic sequence [54].

First, we consider adiabatic rapid passage in a two-level system. The Hamiltonian for a two-level system with states  $|g\rangle$  and  $|r\rangle$ , interacting with a chirped laser pulse (laser frequency and intensity are varied during the pulse), is written as

$$\mathcal{H}_{0}\left(t\right) = \frac{\hbar}{2} \begin{pmatrix} 0 & \Omega_{0}\left(t\right) \\ \Omega_{0}\left(t\right) & 2\delta\left(t\right) \end{pmatrix}. \tag{1}$$

Here  $\Omega_0(t)$  is a time-dependent Rabi frequency and  $\delta(t)$  is a time-dependent detuning from the resonance. The adiabatic evolution of the two-level system is characterized by a mixing angle  $\theta(t)$  [96]:

$$\tan \left[2\theta\left(t\right)\right] = \Omega_0\left(t\right)/\delta\left(t\right). \tag{2}$$

For counterdiabatic driving the time-dependent Rabi frequency is modified as following

$$\Omega(t) = \Omega_0(t) + i\Omega_{\rm CD}(t). \tag{3}$$

Here

$$\Omega_{\rm CD}(t) = 2\dot{\theta}(t) = \frac{\dot{\Omega}_0(t)\delta(t) - \Omega_0(t)\dot{\delta}(t)}{\Omega_0^2(t) + \delta^2(t)}.$$
 (4)

It requires additional imaginary coupling between quantum states of the two-level system which can be achieved by a phase-shifted laser radiation field. As it has been shown in Ref. [54], the imaginary part of the counterdiabatic Hamiltonian can be created using techniques based on Floquet engineering [97]. At the same time, methods of precise manipulation of amplitudes and phases of the driving pulses are nowadays commonly used in experiments with Rydberg atoms [13].

Now we consider the case of Rydberg blockade which results in enhancement of the Rabi frequency. For a two-atom system with two logical states  $|0\rangle$ ,  $|1\rangle$  and Rydberg state  $|r\rangle$  the Hamiltonian has the form

$$\mathcal{H} = \mathcal{H}_c \otimes I + I \otimes \mathcal{H}_t + \mathsf{B}|rr\rangle\langle rr|,\tag{5}$$

where c, t label each of interacting atoms, and

$$\mathcal{H}_{c/t} = \frac{\Omega(t)}{2} |r\rangle_{c/t} \langle 1| + \delta(t) |r\rangle_{c/t} \langle r| + \text{H.c.}$$
.

Here B is a blockade strength. By eliminating the doubly excited Rydberg state  $|rr\rangle$  we reduce this Hamiltonian to a two-level system with states  $|11\rangle$  and  $\frac{1}{\sqrt{2}}(|1r\rangle + |r1\rangle)$  with enhanced coupling  $\sqrt{2}\Omega_0(t)$ . As the counterdiabatic

term in  $\mathcal{H}_{CD}$  will experience the same enhancement, the optimizing counterdiabatic term will be written as

$$\Omega_{CD}^{\text{blockade}}\left(t\right) = \frac{\dot{\Omega}_{0}\left(t\right)\delta\left(t\right) - \Omega_{0}\left(t\right)\dot{\delta}\left(t\right)}{2\Omega_{0}^{2}\left(t\right) + \delta^{2}\left(t\right)},\tag{6}$$

which is different from the Eq. (4). In general, the optimal adiabatic sequences with counterdiabatic driving are different for a single-atom excitation and Rydberg excitation of a two-atom system in a blockade regime [54]. This is certainly an obstacle for implementing of  $C_Z$  gate which requires identical pulse sequences regardless of the initial state of two atoms. This problem was not fully addressed in Refs. [54, 63] where a non-separable driving Hamiltonian for a two-atom system was studied instead of the driving part of the Hamiltonian from the Eq. (5).

Although the authors of Refs. [54, 63] clearly demonstrated advantages of counterdiabatic driving for gate performance, the Hamiltonian obtained by them was not feasible for direct experimental implementation when the initial ground state of the atom is not known.

Surprisingly, we found that it is possible to find the parameters of laser pulses which provide the necessary time dynamics of populations and phases in *both* cases. This makes the design of fast adiabatic gates a simple and robust procedure.

We used the following identical profiles of each laser pulse in the adiabatic sequence

$$\Omega_0(t) = \Omega_{0\max} \left[ \exp\left(-\frac{(t-t_0)^4}{w^4}\right) - a \right] / (1-a) 
\delta(t) = \delta_0 \sin\left(\frac{\pi(t-t_0)}{T}\right).$$
(7)

with  $t_0$  the center of the pulse, and the offset a set to give zero amplitude at the start and stop points. The pulses are centered at  $t_0 = \pm T/2$  and have w = T/4. The counterdiabatic driving term was calculated using Eq. (4) and Eq. (7). The time dependences of the Rabi frequency  $\Omega_0(t)$  and counterdiabatic drive  $\Omega_{CD}(t)$  are shown in Fig. 2(a). The time dependence of the detuning  $\delta(t)$  is shown in Fig. 2(b).

The caclulated time dependences of the populations  $P_{01}$  and  $P_{11}$  of the states  $|01\rangle$  and  $|11\rangle$  respectively are shown in Figs. 2 (c),(d). The time dynamics of the population is governed by different Rabi frequencies  $\Omega_0(t)$ and  $\sqrt{2}\Omega_0(t)$ . Therefore, only one of two conditions, described either by Eq. (4) or by Eq. (6) can be met. We used the counterdiabatic driving term described by Eq. (4) as an ansatz, and optimized the pulse parameters to find the regime when the system with  $\sqrt{2}$  enhanced Rabi frequency also returns to the ground state, as shown in Fig. 1(d). For the pulse shapes defined by Eq. (7) the optimal pulse parameters for gate time 2Tare  $\Omega_{0\text{max}} = 2.003\pi/T$  and  $\delta_0 = \pi/T$ . For coherent laser excitation by a laser pulse with constant Rabi frequency  $\Omega_{0\text{max}}$  during time 2T the condition of a  $2\pi$ -pulse which returns the system to the initial state with a  $\pi$  phase shift

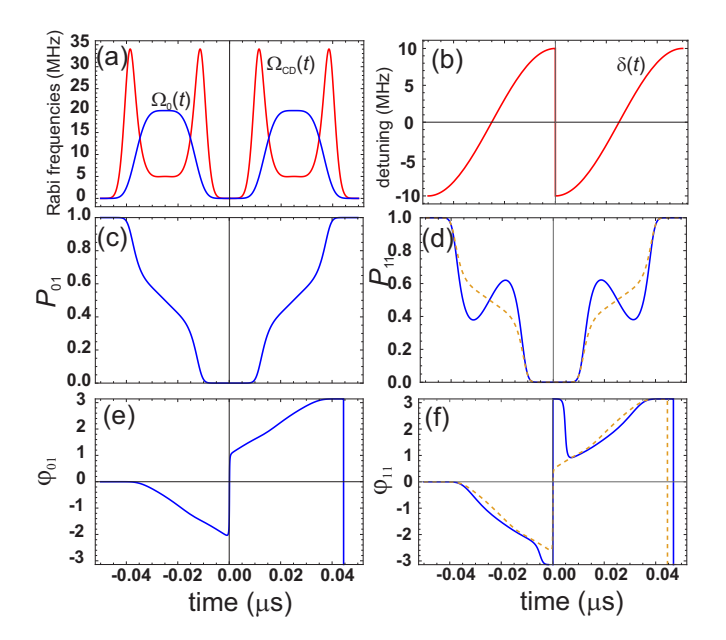


FIG. 2. (color online) (a) Rabi frequency  $\Omega_0(t)$  (blue) and counterdiabatic drive  $\Omega_{CD}(t)$  (red). (b) Detuning  $\delta(t)$ . (c) Population  $P_{01}$  of the ground state  $|01\rangle$ . (d) Population  $P_{11}$  of the ground state  $|11\rangle$  with pulse parameters from Eq. (4) (solid line) and from Eq. (6) (dashed line). (e) Phase  $\varphi_{01}$  of the ground state  $|01\rangle$ . (f) Phase  $\varphi_{11}$  of the ground state  $|11\rangle$  with pulse parameters from Eq. (4) (solid line) and from Eq. (6) (dashed line). The gate time  $2T=0.1~\mu s$  defines Rabi frequency  $\Omega_{0max} = 2\pi/T$  and detuning  $\delta_0 = \pi/T$  of the pulses from Eq. (7), which are centered at  $\pm T/2$  and have w = T/4.

is  $\Omega_{0\mathrm{max}} = \pi/T$ . This sets the theoretical limit for minimal Rabi frequency required for gate operation. We see that in terms of gate performance our proposal is closer to time-optimal protocols [14], being much faster than a purely adiabatic scheme.

The detuning in Eq. (7) can be written as  $\delta(t) = \delta_0 \sin \left[\delta_0(t-t_0)\right]$ . Notably, all properties of laser pulses in our protocol are defined by gate duration only and in the case of perfect blockade the gate is fully scalable for any value of T.

In both cases the  $\pi$  phase shift of the ground state is accumulated, as shown in Figs. 2(e),(f). In contrast to Levine-Pichler [11] and time-optimal [13, 14], our gate does not create undesired phase shifts which require additional single-qubit phase corrections. It is important to note that these parameters do not provide counteradiabatic driving at Rabi frequency  $\sqrt{2}\Omega_0(t)$  which requires the counterdiabatic term to have the form defined in Eq. (6). The population and phase dynamics for true counterdiabatic driving defined by Eq. (6) is shown as dashed lines in Figs. 2(d),(f). Compared to the case of true counterdiabatic driving, it is possible to achieve the necessary population dynamics only in the narrow window of parameters of laser pulses, which resembles more on-resonance laser excitation than adiabatic passage. This reduces the robustness of the proposed protocol, but still allows achievement of high fidelities of entanglement.

To generate entanglement, we start with the state  $|ct\rangle = |00\rangle$ , then apply an ideal Hadamard gate to each qubit, the Rydberg  $C_Z$  operation, and a final Hadamard to one of the qubits which prepares the Bell state  $|B\rangle = (|00\rangle + |11\rangle)/\sqrt{2}$ . The Bell fidelity can be defined as[98]  $\mathcal{F} = (\rho_{0000} + \rho_{1111})/2 + |\rho_{1100}|$ . The sensitivity of the gate fidelity to variation of Rabi frequency and detuning is illustrated as density plot in Fig. 3(a). While not being fully counterdiabatic, our gate protocol is tolerant to minor variation of the pulse parameters, although it is in general more sensitive to them than the previously developed fully adiabatic scheme [21].

We compared the sensitivity of Bell fidelity to the variation of Rabi frequency of the laser pulse for three schemes of  $C_Z$  gate scaled to the same gate time 2T = $0.1 \,\mu s$ . The dependence of Bell infidelity on the ratio between the Rabi frequency of the driving pulse  $\Omega_0$ and the optimal value of the Rabi frequency for each gate scheme  $\Omega_0^{\rm opt}$  is shown in Fig. 3(b). For the adiabatic scheme  $\Omega_0^{\rm opt}=20.03\,{\rm MHz}$ . For Levine-Pichler gate with duration  $2T = 0.1 \,\mu\text{s}$  we used Rabi frequency  $\Omega_0^{\text{opt}}/(2\pi) = 4.29268/(2\pi T) = 13.664 \,\text{MHz}$ , Rydberg detuning  $\delta_0/(2\pi) = 0.377371/(2\pi)\,\mathrm{MHz}$  and phase shift 3.90242 at the center of the laser pulse [11]. The time-optimal scheme has the following parameters [13]:  $\Omega_0^{\text{opt}}/(2\pi) = 1.215/(2T) = 12.15 \,\text{MHz}$  and the phase profile of the laser pulse is  $\varphi(t) = A\cos[w(t+T) - \varphi_0]$  with  $A/(2\pi) = 0.1122$ , w = 1.0431 $\Omega_0$  and  $\varphi_0 = -0.7318$ . Although our scheme requires slightly higher value of the Rabi frequency compared to other schemes, it demonstrates the smallest sensitivity of Bell infidelity to variation of the Rabi frequency of the driving field. This is potentially advantageous, as precise control of laser intensity in the experiment is a difficult technical task.

The finite blockade strength B is also a well-known source of infidelities of entangling gates with neutral atoms. To estimate its contribution to the gate error budget, we calculated the dependence of the Bell infidelity on the blockade strength for optimized laser pulse parameters, without taking into account finite lifetimes of atomic states and other sources of errors. The dependence, shown in Fig. 3(c), shows that with  $B/(2\pi) > 2$  GHz, the infidelity due to finite blockade error goes below  $10^{-4}$ .

### III. SINGLE-PHOTON ADIABATIC RAPID PASSAGE

To analyze the gate performance taking into account finite lifetimes of Rydberg states, we used a two-atom master equation in Lindblad form with the Hamiltonian from Eq. (5), similar to the approach from the previous work [21]:

$$\frac{d\rho}{dt} = i[\mathcal{H}, \rho] + \mathcal{L}[\rho] \tag{8}$$

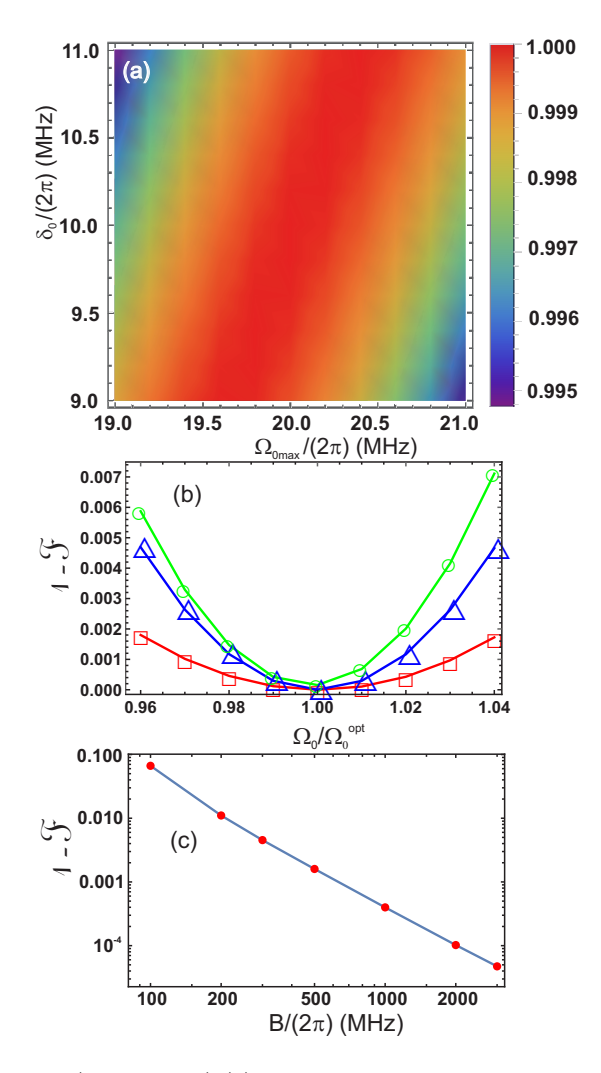


FIG. 3. (color online) (a) Density plot of Bell fidelity as function of Rabi frequency  $\Omega_{0\max}$  and detuning  $\delta_0$ . (b) Dependence of Bell state infidelity on the ratio between the driving Rabi frequency  $\Omega_0^{\rm opt}$ , separately calculated for each  $C_Z$  scheme for the gate time  $2T=0.1\,\mu{\rm s}$ : our gate scheme (squares), Levine-Pichler gate (triangles) and time-optimal gate (circles). (c) Dependence of Bell state infidelity using  $C_Z$  gate with ARP pulses on blockade strength B.

Here the initial conditions are  $\rho(0) = \rho_c(0) \otimes \rho_t(0)$  where c, t label each of interacting atoms.

The decay term is

$$\mathcal{L}[\rho] = \sum_{\ell=c.t} \sum_{j=0.1,d} L_j^{(\ell)} \rho L_j^{(\ell)}^\dagger - \frac{1}{2} L_j^{(\ell)}^\dagger L_j^{(\ell)} \rho - \frac{1}{2} \rho L_j^{(\ell)}^\dagger L_j^{(\ell)}$$

with  $L_j^{(\ell)} = \sqrt{b_{jr}\gamma_r}|j\rangle_{\ell}\langle r|$  where  $\gamma_r = 1/\tau_r$  is the population decay rate of the Rydberg state and the  $b_{jr}$  are branching ratios to lower level j.

The energy level scheme for this model is shown in Fig. 4(a). The levels  $|0\rangle, |1\rangle$  are the logical states which can be hyperfine energy sublevels of the ground state of cesium or rubidium atoms. The uncoupled state  $|d\rangle$ 

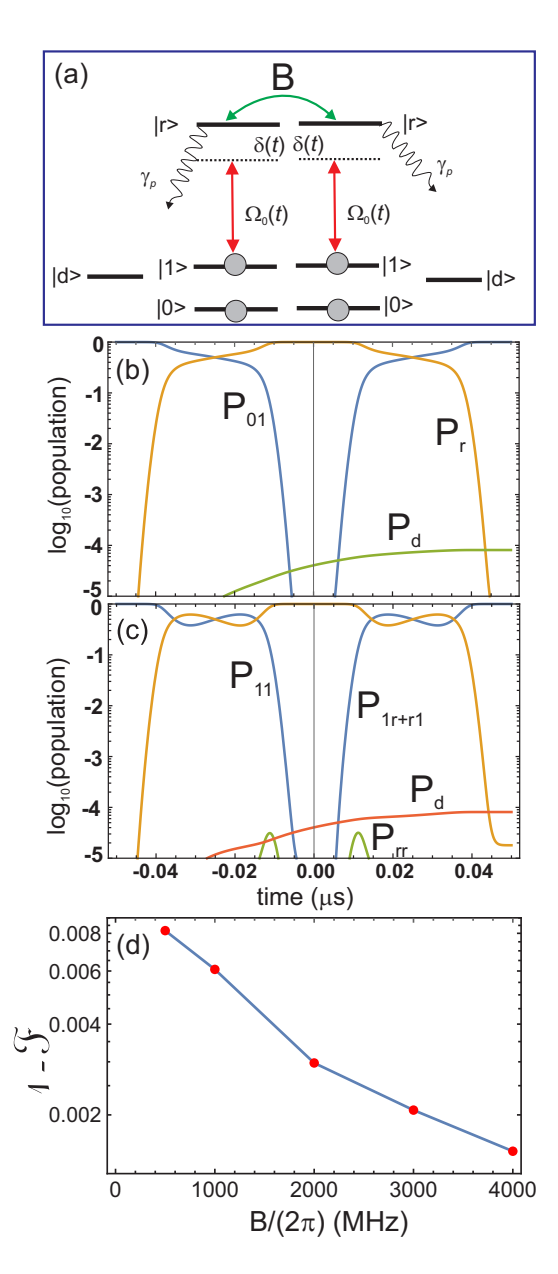


FIG. 4. (color online) (a) Scheme of the atomic energy levels used in numeric simulation. (b) Populations of the  $|10\rangle$ ,  $|r0\rangle$  and  $|d\rangle$  states for the initial state  $|10\rangle$ . The population in  $|d\rangle$  is defined as  $1 - \text{Tr}_{0,1,r}[\rho]$ . (c) Populations of the  $|11\rangle$ ,  $|1r\rangle + |r1\rangle$ ,  $|rr\rangle$  and  $|d\rangle$  states for the initial state  $|11\rangle$ . (d) Dependence of infidelity of Bell state on blockade strength B.

represents all the ground hyperfine states outside the qubit basis. We assume that all population leakage into  $|d\rangle$  is an uncorrectable error. For comparison with the previous proposal we use the atomic parameters for Cs  $107p_{3/2}$  state which are  $\gamma_r=1/(540~\mu\text{s})~b_{dr}=7/8$ ,  $b_{0r}=b_{1r}=1/16~[67,99]$ . We use the same time profiles of Rabi frequency and detunings as in Fig. 2. The population of ground and excited states are shown in Fig. 4 (b) and (c) for initial states  $|01\rangle$  and  $|11\rangle$ , respectively at B/ $(2\pi)=4$  GHz. In both cases the system returns back to the ground state after an effective  $2\pi$  rotation.

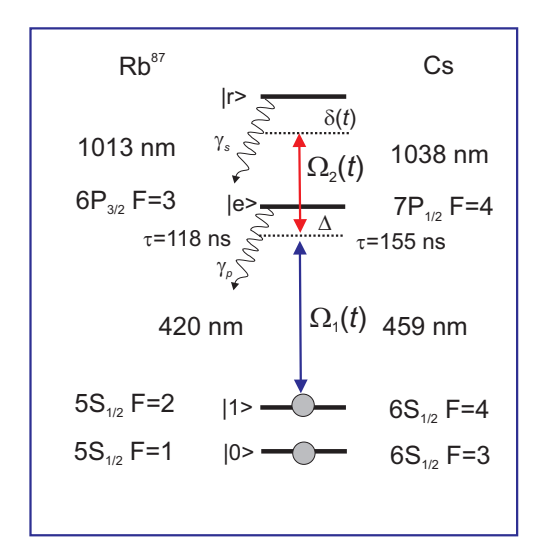


FIG. 5. (color online) Scheme of two-photon Rydberg excitation in Cs and Rb atoms with Rabi frequencies  $\Omega_1(t), \Omega_2(t)$  via intermediate state  $|p\rangle$  at detuning  $\Delta$ .

This scheme of a single-photon adiabatic rapid passage gives us an upper limit of the fidelity of the proposed gate protocol for a room-temperature environment. The gate duration here is approximately five times shorter than in the previous work [21]. From the simulation of the generation of Bell state we obtained the Bell fidelity  $\mathcal{F}=0.9999$  for blockade strength B/( $2\pi$ ) = 4 GHz which is limited by lifetime of a Rydberg state.

For Rb<sup>87</sup> the  $113p_{3/2}$  state has similar lifetime, but the branching ratios are  $b_{dr}=3/4$ ,  $b_{0r}=b_{1r}=1/8$ . However, in the calculations we have not found any substantial differences in the gate performance between Rb and Cs. The fidelity  $\mathcal{F}=0.9999$  is reached at the same blockade strength B/ $(2\pi)=4$  GHz.

### IV. $C_Z$ GATE WITH TWO-PHOTON ADIABATIC RAPID PASSAGE

Two-photon schemes of Rydberg excitation, shown in Fig. 5, are most common in the experiments with highfidelity gates for ultracold neutral atoms [11, 13, 100]. For rubidium, the ground-state  $|5S\rangle$  atoms are excited through the intermediate  $|6P_{3/2}\rangle$  state to Rydberg nS or nD states using laser fields with 420 nm and 1013 nm wavelengths at first and second excitation steps, respectively [11]. For cesium with  $|6S\rangle$  ground state the excitation path goes through the intermediate  $|7P_{1/2}\rangle$  state using laser radiation at 459 nm and 1038 nm at first and second excitation steps, respectively [100]. The commonly used technique for adiabatic laser excitation in three-level systems is STIRAP [89]. Shortcut to adiabatic passage for STIRAP requires additional coupling between first and third energy levels [101] which is challenging in ladder schemes used for Rydberg excitation. Therefore instead we consider a two-photon adiabatic passage, which

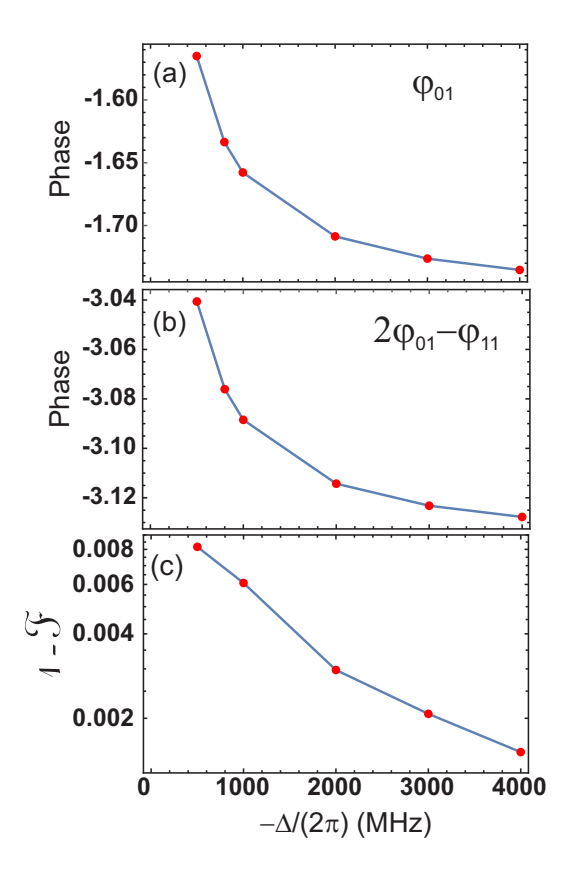


FIG. 6. (color online) (a) Dependence of the phase shift  $\phi_{01}$  of the ground state  $|01\rangle$  on the detuning  $-\Delta$ . (b) Dependence of the  $C_Z$  phase shift written as  $2\phi_{01} - \phi_{11}$  on the detuning  $-\Delta$ . (c) Dependence of infidelity of Bell state on the detuning  $-\Delta$  at  $B/(2\pi)=1$  GHz.

recently attracted interest for quantum information processing with Rydberg atoms [35].

In order to suppress the spontaneous decay from the intermediate excited states, large detuning  $\Delta$  of order of several GHz is required [13]. In this case the intermediate excited state can be adiabatically eliminated, and the three-level system is reduced to a two-level system with a Rabi frequency  $\Omega_{\text{two-photon}} = \Omega_1 \Omega_2 / 2\Delta$ , where  $\Omega_1$  and  $\Omega_2$  are the Rabi frequencies of the first and second excitation steps, respectively and  $\Delta$  is the detuning from the intermediate excited state. However, when  $\Omega_1 \neq \Omega_2$ , there is an additional light shift of the two-photon resonance [86]. For complex time-dependent profiles of laser pulses required for counterdiabatic driving the compensation of this light shift is not straightforward. Therefore we consider identical profiles of the Rabi frequencies  $\Omega_1$  and  $\Omega_2$ .

The calculated fidelities are slightly higher when the sign of  $\Delta$  in the Hamiltonian is opposite to the sign of the blockade shift B, i.e.  $\Delta$  should be negative for the context considered in the present work.

We used identically shaped pulses designed in such a way that  $\Omega_{\text{two-photon}}$  has same profile as in Eqs. (4), (3).

$$\Omega_1(t) = \Omega_2(t) = \sqrt{-2\Delta(\Omega_0(t) + i\Omega_{\rm CD}(t))}.$$
 (9)

However, due to the finite value of  $\Delta$  there is an additional phase shift at single-atom excitation, compared to the phases shown in Fig. 2(e),(f). The numerically calculated phase shift  $\phi_{01}$  accumulated after returning to the ground state (instead of expected  $\pi$  phase shift) for the initial  $|01\rangle$  state is shown in Fig. 6(a). To create Bell state, this phase shift must be corrected after the end of the gate using additional single-qubit phase gates. The difference  $2\phi_{01}-\phi_{11}$  shown in Fig. 6(b) (which should be equal to  $\pm\pi$  in ideal case) illustrates the gate performance. In these calculations we considered an infinite blockade strength. However, we find that even for large  $\Delta=-4$  GHz there is still a small residual phase error.

For the analysis of Bell fidelity we used the model of two-photon Rydberg excitation adopted from the previous work [21] with modified Eq.(8)

$$\mathcal{H}_{c/t} = \frac{\Omega_{1}(t)}{2} |p\rangle_{c/t} \langle 1| + \frac{\Omega_{2}(t)}{2} |r\rangle_{c/t} \langle p|$$

$$+ \Delta |p\rangle_{c/t} \langle p| + \delta(t) |r\rangle_{c/t} \langle r| + \text{H.c.}.$$

and

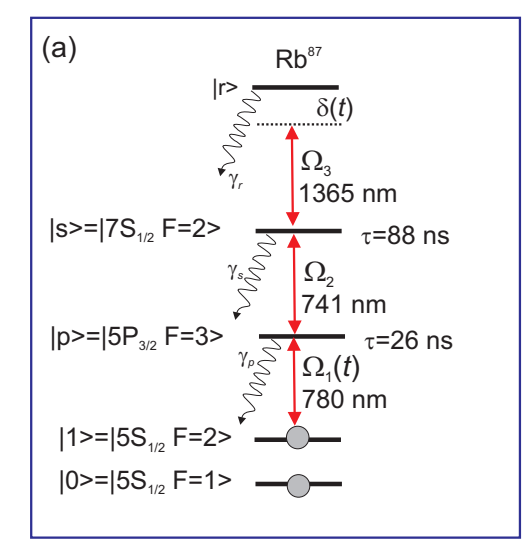
$$\mathcal{L}[\rho] = \sum_{\ell=c,t} \sum_{j,k=0,1,d,p,r} L_{jk}^{(\ell)} \rho L_{jk}^{(\ell)^{\dagger}} - \frac{1}{2} L_{jk}^{(\ell)^{\dagger}} L_{jk}^{(\ell)} \rho - \frac{1}{2} \rho L_{jk}^{(\ell)^{\dagger}} L_{jk}^{(\ell)}$$

where  $L_{jk}^{(\ell)} = \sqrt{b_{jk}\gamma_k}|j\rangle_\ell\langle k|$  for j < k and 0 otherwise. The calculated Bell infidelity for two-photon excitation scheme at B/(2 $\pi$ )=1 GHz is shown in Fig. 6(c). The fidelity reaches  $\mathcal{F} = 0.998$  for  $\Delta/(2\pi) = 4$  GHz.

## V. THREE-PHOTON ADIABATIC RAPID PASSAGE

Recently we proposed a scheme of high-fidelity individual addressing at Rydberg excitation using three-photon transitions between ground and Rydberg state by three lasers with Rabi frequencies  $\Omega_1$ ,  $\Omega_2$ ,  $\Omega_3$ , as shown in Fig. 7(a) [102]. If  $\Omega_2 \gg \Omega_1, \Omega_3$ , even when all three lasers are tuned to the exact resonances with all three transitions, the intermediate excited states are not populated and the coherent excitation of Rydberg atoms occurs, with the effective Rabi frequency  $\Omega_{\text{three-photon}} =$  $\Omega_1\Omega_3/\Omega_2$ . In this case it is possible to compensate for the influence of the inhomogeneity of the tightly focused laser beams on the value of  $\Omega_{\text{three-photon}}$ , which opens the way to the individual addressing when performing entangling gates in atomic arrays [102]. Another advantage of a three-photon scheme is the ability to completely eliminate the Doppler shift of the resonance by geometric arrangement of three laser beams which excite Rydberg atoms [103]. The single-atom three-photon Rabi oscillations were recently experimentally demonstrated in our work [104].

In contrast to the two-photon scheme of laser excitation, the three-photon resonance is not shifted even when all three Rabi frequencies are different [102]. Therefore



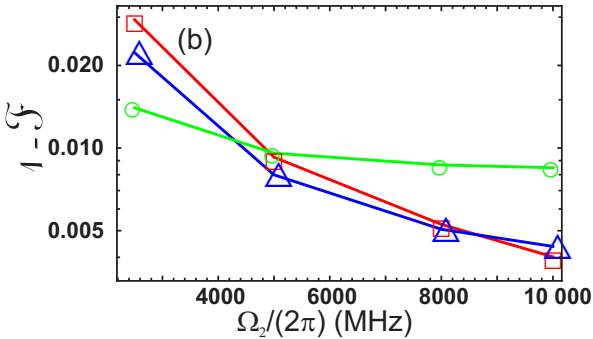


FIG. 7. (color online) (a) Scheme of three-photon Rydberg excitation for Rb<sup>87</sup> atoms. (b) Dependence of infidelity of Bell state for counterdiabatic driving (squares), Levine-Pichler gate (triangles) and time-optimal gate (circles) at three-photon Rydberg excitation on the Rabi frequency  $\Omega_2$  of the intermediate transition at B/( $2\pi$ )=1 GHz.

it is possible to implement counterdiabatic driving by shaping the phase profile of only one laser beam. We apply the time-dependent detuning  $\delta(t)$  to the third step of laser excitation and the profile of the first step pulse is modified to include the counterdiabatic driving term. We use constant values of  $\Omega_2$  and  $\Omega_3$  and the following profile of  $\Omega_1(t)$ :

$$\Omega_{1}(t) = \frac{\Omega_{2}}{\Omega_{3}} \left[ \Omega_{0}(t) + i\Omega_{CD}(t) \right]. \tag{10}$$

For analysis of the gate perfomance we solved the master equation with the Hamiltonian

$$\mathcal{H}_{\mathrm{c/t}} = \frac{\Omega_{1}(t)}{2} |p\rangle_{\mathrm{c/t}} \langle 1| + \frac{\Omega_{2}}{2} |s\rangle_{\mathrm{c/t}} \langle p| + \frac{\Omega_{3}}{2} |r\rangle_{\mathrm{c/t}} \langle s| + \delta(t) |r\rangle_{\mathrm{c/t}} \langle r| + \mathrm{H.c.}$$

and

$$\mathcal{L}[\rho] = \sum_{\ell=c,t} \sum_{j,k=0,1,d,p,s,r} L_{jk}^{(\ell)} \rho L_{jk}^{(\ell)\dagger} - \frac{1}{2} L_{jk}^{(\ell)\dagger} L_{jk}^{(\ell)} \rho - \frac{1}{2} \rho L_{jk}^{(\ell)\dagger} L_{jk}^{(\ell)} \text{terdiabatic driving demonstrates performance, comparable with modern entangling gate protocols.}$$

where 
$$L_{jk}^{(\ell)} = \sqrt{b_{jk}\gamma_k}|j\rangle_{\ell}\langle k|$$
 for  $j < k$  and 0 otherwise.

We have found that for three-photon adiabatic passage higher fidelities are obtained for longer pulse durations  $T=0.1~\mu s$  compared to the cases, previously considered in this work. We taken the parameters of laser pulses  $\Omega_{0\text{max}}/(2\pi) = 10 \text{ MHz and } \delta_0/(2\pi) = 5 \text{ MHz in Eq. (7)},$ while keeping  $\Omega_3/(2\pi) = 250$  MHz. The calculated Bell fidelity at  $B/2\pi = 1$  GHz is shown as squares in Fig. 7(b). For three-photon laser excitation the intermediate Rabi frequency  $\Omega_2$  plays the role of effective detuning. With increase of  $\Omega_2$  the populations of the intermediate excited states become smaller due to AC Stark splitting of the resonance [102]. Therefore, we expected the increase of Bell fidelity for larger values of  $\Omega_2$ , which is confirmed by the calculations in Fig. 7(b). For three-photon gate protocol we obtain Bell fidelity  $\mathcal{F} = 0.996$  at  $\Omega_2/(2\pi) =$ 10 GHz and  $B/(2\pi) = 1$  GHz.

We also simulated the performance of a symmetric Levine-Pichler  $C_Z$  gate protocol, using collective Rabi frequency, Rydberg detuning and phase shift from Ref. [11], but applying these parameters to a threephoton excitation scheme after adiabatic elimination of the intermediate excited states. We used time-dependent profile of  $\Omega_1(t)$  with a phase shift  $\Delta \psi = 3.90242$  at the center of the laser pulse, half of the gate time T= $0.429268 \,\mu s$  and detuning of the third step laser from the three-photon resonance  $\delta/(2\pi) = 3.77371/(2\pi)$  MHz. We fixed the value of the Rabi frequency at the third step of laser excitation  $\Omega_3/(2\pi) = 100$  MHz, which provided us the best fidelity for this gate scheme, and the blockade strength  $B/2\pi = 1$  GHz. In this case we obtained a similar dependence of Bell fidelity on the intermediate Rabi frequency  $\Omega_2$ , which is shown by triangles in Fig. 7(b).

Similarly, we considered the parameters of the timeoptimal gate from [13] for simulation of the gate performance at three-photon laser excitation. For time-optimal gate the best results in our simulations are obtained using fixed Rabi frequencies at first [with  $\Omega_1/(2\pi) = 100 \text{ MHz}$ ] and second steps of laser excitation, while the phase of the laser pulse at the third step is time-dependent. Following Ref. [13] we used collective Rabi frequency  $\Omega_0/(2\pi) = 4.6$  MHz, gate time  $2T/(2\pi) = 1.215/\Omega_0$  and time dependence of the phase of the third step of laser excitation  $\varphi(t) = A\cos\left[w(t+T) - \varphi_0\right]$  with  $A/(2\pi) =$ 0.1122, w =  $1.0431\Omega_0$  and  $\varphi_0 = -0.7318$ . Results of simulation are shown as green circles in Fig. 7(b). The time-optimal gate demonstrated higher fidelity at smaller values of intermediate Rabi frequency. Both adiabatic and Levine-Pichler gates outperform the time-optimal protocol with increase of  $\Omega_2$ . Smooth shapes of laser pulses used in our approach have potential advantage for robustness of gate schemes which exploit multi-photon transitions [13]. From Fig. 7 we can conclude that even for complex three-photon Rydberg excitation the coun-

#### VI. CONCLUSION

In summary, we have revised the scheme of symmetric  $C_Z$  gate based on double adiabatic passage at Rydberg excitation using counterdiabatic driving. This allowed us to substantially reduce the gate operation time with moderate increase of the Rabi frequency without the need for substantially larger Rydberg blockade strengths. All parameters of laser pulses of our  $C_Z$  gate for a general scheme of single-photon laser excitation depend on a single parameter which is gate duration time. The main advantages of our scheme are the following: (i) it is almost as fast, as modern time-optimal and Levine-Pichler gate protocols, but has reduced sensitivity of the Bell state fidelity to the variation of laser intensity; (ii) similarly to the previously designed double adiabatic sequence, it does not create undesired single-qubit phase shifts; (iii) the profiles of laser pulses are described analytically without the need to use many parameters obtained from sophisticated numeric optimization.

The upper limit of Bell fidelity at room temperature for the simplest single-photon excitation scheme is found to be  $\mathcal{F}=0.9999$ . This can be useful for future applications of quantum error correction with ultracold neutral atoms. In the calculation of this limit we have taken into account only finite blockade strength and lifetimes of Rydberg states. These limitations are intrinsic and unavoidable, in contrast to technical imperfections of the experiment, including laser phase noise and finite temperature of the atoms. The account of the technical factors to the gate error budget should be calculated separately, and it

strongly depends on the state of art of the experimental technology. In the previous work [21] the validity of our physical model was discussed in detail.

We also applied our gate scheme to two-photon and three-photon configurations of laser excitation. The Bell fidelity in these schemes is affected by finite lifetimes of the intermediate excited states and non-adiabatic transitions which limit the applicability of adiabatic elimination of the intermediate levels. However, we have shown that high fidelities of entanglement can be achieved in these more complex configurations. We also considered the Levine-Pichler and time-optimal gate protocols for three-photon laser excitation scheme and compared them with our pulse sequence and found comparable performance for optimal pulse parameters.

The potential advantages of three-photon laser excitation are the ability for complete compensation of the Doppler shift of the resonance at Rydberg excitation and the possibility for individual addressing in the atomic arrays. In our calculations both single-photon and two-photon laser excitation schemes slightly outperform the three-photon excitation in terms of overall fidelity. However, the flexibility of three-photon excitation because of absence of light shifts and additional undesired single-qubit phase shifts, which are typical for two-photon excitation schemes, is clearly seen from the calculations.

### ACKNOWLEDGMENTS

This work was supported by the Russian Science Foundation Grant No. 23-42-00031 https://rscf.ru/en/project/23-42-00031/.

- N.-C. Chiu, E. C. Trapp, J. Guo, M. H. Abobeih, L. M. Stewart, S. Hollerith, P. Stroganov, M. Kalinowski, A. A. Geim, S. J. Evered, S. H. Li, L. M. Peters, D. Bluvstein, T. T. Wang, M. Greiner, V. Vuletic, and M. D. Lukin, Nature (2025).
- [2] H. J. Manetsch, G. Nomura, E. Bataille, K. H. Leung, X. Lv, and M. Endres, arXiv.2403.12021 10.48550/arXiv.2403.12021 (2024).
- [3] T. M. Graham, Y. Song, J. Scott, C. Poole, L. Phuttitarn, K. Jooya, P. Eichler, X. Jiang, A. Marra, B. Grinkemeyer, M. Kwon, M. Ebert, J. Cherek, M. T. Lichtman, M. Gillette, J. Gilbert, D. Bowman, T. Ballance, C. Campbell, E. D. Dahl, O. Crawford, T. Noel, and M. Saffman, Nature 604, 457 (2022).
- [4] S. Ebadi, A. Keesling, M. Cain, T. T. Wang, H. Levine, D. Bluvstein, G. Semeghini, A. Omran, J.-G. Liu, R. Samajdar, et al., Science 376, 1209 (2022).
- [5] A. G. de Oliveira, E. Diamond-Hitchcock, D. M. Walker, M. T. Wells-Pestell, G. Pelegrí, C. J. Picken, G. P. A. Malcolm, A. J. Daley, J. Bass, and J. D. Pritchard, PRX Quantum 6, 010301 (2025).
- [6] D. Bluvstein, S. J. Evered, A. A. Geim, S. H. Li, H. Zhou, T. Manovitz, S. Ebadi, M. Cain, M. Kalinowski, D. Hangleiter, J. P. B. Ataides, N. Maskara, I. Cong, X. Gao, P. S. Rodriguez, T. Karolyshyn, G. Se-

- meghini, M. J. Gullans, M. Greiner, V. Vuletic, and M. D. Lukin, Nature **626**, 58 (2024).
- [7] X. Li, J.-Y. Hou, J.-C. Wang, G.-W. Wang, X.-D. He,
   F. Zhou, Y.-B. Wang, M. Liu, J. Wang, P. Xu, and M.-S. Zhan, arXiv:2411.08502 10.48550/arXiv.2411.08502 (2024).
- [8] R. B.-S. Tsai, X. Sun, A. L. Shaw, R. Finkelstein, and M. Endres, Phys Rev X Quantum 6, 010331 (2025).
- [9] D. Bluvstein, A. A. Geim, S. H. Li, S. J. Evered, J. P. B. Ataides, G. Baranes, A. Gu, T. Manovitz, M. Xu, M. Kalinowski, S. Majidy, C. Kokail, N. Maskara, E. C. Trapp, L. M. Stewart, S. Hollerith, H. Zhou, M. J. Gullans, S. F. Yelin, M. Greiner, V. Vuletic, M. Cain, and M. D. Lukin, arXiv:2506.20661 10.48550/arXiv.2506.20661 (2025).
- [10] D. Jaksch, J. I. Cirac, P. Zoller, S. L. Rolston, R. Côté, and M. D. Lukin, Phys. Rev. Lett 85, 2208 (2000).
- [11] H. Levine, A. Keesling, G. Semeghini, A. Omran, T. T. Wang, S. Ebadi, H. Bernien, M. Greiner, V. Vuletić, H. Pichler, and M. D. Lukin, Phys. Rev. Lett. 123, 170503 (2019).
- [12] Z. Fu, P. Xu, Y. Sun, Y. Liu, X. He, X. Li, M. Liu, R. Li, J. Wang, L. Liu, and M. Zhan, Phys. Rev. A 105, 042430 (2021).
- [13] S. J. Evered, D. Bluvstein, M. Kalinowski, S. Ebadi,

- T. Manovitz, H. Zhou, S. H. Li, A. A. Geim, T. T. Wang, N. Maskara, H. Levine, G. Semeghini, M. Greiner, V. Vuletic, and M. D. Lukin, Nature **622**, 268 (2023).
- [14] S. Jandura and G. Pupillo, Quantum 6, 712 (2022).
- [15] M. G. Bason, M. Viteau, N. Malossi, P. Huillery, E. Arimondo, D. Ciampini, R. Fazio, V. Giovannetti, R. Mannella, and O. Morsch, Nat. Phys. 8, 147 (2012).
- [16] T. H. Chang, T. Wang, H. Jen, and Y.-C. Chen, New J. Phys. 25, 123007 (2023).
- [17] G. Giudici, S. Veroni, G. Giudice, H. Pichler, and J. Zeiher, PRX Quantum 6, 030308 (2025).
- [18] Y. Ming, Z.-X. Fu, and Y.-X. Du, arXiv:2412.19193 10.48550/arXiv.2412.19193 (2024).
- [19] C. Fromonteil, D. Bluvstein, and H. Pichler, PRX Quantum 4, 020335 (2023).
- [20] I. I. Beterov, M. Saffman, E. A. Yakshina, D. B. Tretyakov, V. M. Entin, S. Bergamini, E. A. Kuznetsova, and I. I. Ryabtsev, Phys. Rev. A 94, 062307 (2016).
- [21] M. Saffman, I. I. Beterov, A. Dalal, E. J. Páez, and B. C. Sanders, Phys. Rev. A 101, 062309 (2020).
- [22] X. Wu, X. Liang, Y. Tian, F. Yang, C. Chen, Y.-C. Liu, M. K. Tey, and L. You, Chinese Physics B 30, 020305 (2021).
- [23] Y. Wu, S. Kolkowitz, S. Puri, and J. D. Thompson, Nature Communications 13, 4657 (2022).
- [24] M. Morgado and S. Whitlock, AVS Quantum Science 3, 023501 (2021).
- [25] A. Pagano, S. Weber, D. Jaschke, T. Pfau, F. Meinert, S. Montangero, and H. P. Büchler, Phys. Rev. Res. 4, 033019 (2022).
- [26] S. Jandura, J. D. Thompson, and G. Pupillo, PRX Quantum 4, 020336 (2023).
- [27] Z. Fu, P. Xu, Y. Sun, Y. Liu, X. He, X. Li, M. Liu, R. Li, J. Wang, L. Liu, and M. Zhan, Physical Review A 105, 042430 (2022).
- [28] X.-F. Shi, Quantum Science and Technology 7, 023002 (2022).
- [29] M. Mohan, R. de Keijzer, and S. Kokkelmans, Phys. Rev. Res. 5, 033052 (2023).
- [30] C. Poole, T. M. Graham, M. A. Perlin, M. Otten, and M. Saffman, Phys. Rev. A 111, 022433 (2025).
- [31] A. P. Burgers, S. Ma, S. Saskin, J. Wilson, M. A. Alarcón, C. H. Greene, and J. D. Thompson, PRX Quantum 3, 020326 (2022).
- [32] P.-Y. Song, J.-F. Wei, P. Xu, L.-L. Yan, M. Feng, S.-L. Su, and G. Chen, Phys. Rev. A 109, 022613 (2024).
- [33] C. Fromonteil, R. Tricarico, F. Cesa, and H. Pichler, Phys. Rev. Res. 6, 033333 (2024).
- [34] C. Dlaska, K. Ender, G. B. Mbeng, A. Kruckenhauser, W. Lechner, and R. van Bijnen, Phys. Rev. Lett. 128, 120503 (2022).
- [35] G. Pelegri, A. J. Daley, and J. D. Pritchard, Quantum Sci. Technol. 7, 045020 (2022).
- [36] F. Robicheaux, T. M. Graham, and M. Saffman, Phys. Rev. A 103, 022424 (2021).
- [37] J.-L. Wang, Wu, Υ. J.-X. Han. S.-Xia, Υ. Jiang, L. Su, Υ. and J. Song, Phys. Rev. A 103, 012601 (2021).
- [38] W.-X. Li, J.-L. Wu, S.-L. Su, and J. Qian, Phys. Rev. A 109, 012608 (2024).
- [39] M. Li, F.-Q. Guo, Z. Jin, L.-L. Yan, E.-J. Liang, and S.-L. Su, Phys. Rev. A 103, 062607 (2021).
- [40] X. Li, X. Shao, and W. Li,

- Phys. Rev. Appl. 18, 044042 (2022).
- [41] R. Li, J. Qian, and W. Zhang, Quantum Sci. Technol 8, 035032 (2023).
- [42] V. Buchemmavari, S. Omanakuttan, Y.-Y. Jau, and I. Deutsch, Phys. Rev. A 109, 012615 (2024).
- [43] R. Li, S. Li, D. Yu, J. Qian, and W. Zhang, Phys. Rev. Appl. 17, 024014 (2022).
- [44] Y. Liu, Y. Sun, Z. Fu, P. Xu, X. Wang, X. He, J. Wang, and M. Zhan, Phys. Rev. Appl. 15, 054020 (2021).
- [45] M. Xue, S. Xu, X. Li, and X. Li, Phys. Rev. A 110, 032619 (2024).
- [46] X. X. Li, J. B. You, X. Q. Shao, and W. Li, Phys. Rev. A 105, 032417 (2022).
- [47] F. Petiziol, F. Mintert, and S. Wimberger, Europhysics Letters 145, 15001 (2024).
- [48] A. Rodriguez-Blanco, K. B. Whaley, and A. Bermudez, Phys. Rev. A 107, 052409 (2023).
- [49] F.-Q. Guo, J.-L. Wu, X.-Y. Zhu, Z. Jin, Y. Zeng, S. Zhang, L.-L. Yan, M. Feng, and S.-L. Su, Phys. Rev. A 102, 062410 (2020).
- [50] J.-F. Wei, F.-Q. Guo, D.-Y. Wang, Y. Jia, L.-L. Yan, M. Feng, and S.-L. Su, Phys. Rev. A 105, 042404 (2022).
- [51] S. Xu, X. Li, X. Li, J. Li, and M. Xue, Phys. Rev. A 110, 023108 (2024).
- [52] A. Mitra, S. Omanakuttan, M. J. Martin, G. W. Biedermann, and I. H. Deutsch, Phys. Rev. A 107, 062609 (2023).
- [53] Q.-L. Hou, H. Wang, and J. Qian, Phys. Rev. Appl. 22, 034054 (2024).
- [54] L. S. Y. Bosch, T. Ehret, F. Petiziol, E. Arimondo, and S. Wimberger, Annalen der Physik 535, 2300275 (2023).
- [55] G. Doultsinos and D. Petrosyan, Phys. Rev. Res. 7, 023246 (2025).
- [56] J.-L. Wu, Y. Wang, J.-X. Han, S. L. Su, Y. Xia, J. Song, and Y. Jiang,
   Advanced Quantum Technologies 5, 2200042 (2022).
- [57] X.-Q. Shao, Phys. Rev. A 102, 053118 (2020).
- [58] X.-F. Shi, Phys. Rev. A 104, 042422 (2021).
- [59] M. Mohan, J. de Hond, and S. Kokkelmans, Phys. Rev. Appl. 23, 054074 (2025).
- [60] F. Q. Guo, S.-L. Su, W. Li, and X. Q. Shao, Phys. Rev. A 111, 022420 (2025).
- [61] I. R. Sola, S. Shin, and B. Y. Chang, Phys. Rev. A 109, 052603 (2024).
- [62] I. R. Sola, S. Shin, and B. Y. Chang, Phys. Rev. A 108, 032620 (2023).
- [63] L. S. Y. Bosch and S. Wimberger,
  Annalen der Physik 2025, e00163 (2025).
  [64] I. Vybornyi, L. Gerasimov, D. Kupriyanov,
- [64] I. Vybornyi, L. Gerasimov, D. Kupriyanov,
   S. Straupe, and K. Tikhonov,
   Journal of the Optical Society of America B 41, 134 (2023).
- [65] M. Delvecchio, F. Petiziol, E. Arimondo, and S. Wimberger, Phys. Rev. A 105, 042431 (2022).
- [66] A. Dalal and B. C. Sanders, Phys. Rev. A 107, 012605 (2023).
- [67] I. I. Beterov, I. I. Ryabtsev, D. B. Tretyakov, and V. M. Entin, Phys. Rev. A 79, 052504 (2009).
- [68] M. V. Berry, Journal of Physics A: Mathematical and Theoretical 4
- [59] T. Hatomura, J. Phys. B: At. Mol. Opt. Phys. 57, 57 102001 (2024)
- [70] E. Torrontegui, S. Ibuez, S. Martinez-Garaot,
   M. Modugno, A. del Campo, D. Gu?ry-Odelin,
   A. Ruschhaupt, X. Chen, and J. G. Muga, in

- Advances in Atomic, Molecular, and Optical Physics, Advances In Atomic, Molecular, and Optical Physics, Vol. 62, edited by E. Arimondo, P. R. Berman, and C. C. Lin (Academic Press, 2013) pp. 117–169.
- [71] X. Chen, A. Ruschhaupt, S. Schmidt, A. del Campo, D. Guéry-Odelin, and J. G. Muga, Phys. Rev. Lett. 104, 063002 (2010).
- [72] S. Morawetz and A. Polkovnikov, arXiv:2503.01952 10.48550/arXiv.2503.01952 (2025).
- [73] C. L. Latune, D. Sugny, and S. Guerin, arXiv:2503.20130 10.48550/arXiv.2503.20130 (2025).
- [74] D. Guéry-Odelin, A. Ruschhaupt, A. Kiely, E. Torrontegui, S. Martínez-Garaot, and J. G. Muga, Rev. Mod. Phys. 91, 045001 (2019).
- [75] S. An, D. Lv, A. del Campo, and K. Kim, Nature Communications 7, 12999 (2016).
- [76] J. R. Finzgar, S. Notarnicola, M. Cain, M. D. Lukin, and D. Sels, arXiv:2503.01958 10.48550/arXiv.2503.01958 (2025).
- [77] L. Romanato, N. Eshaqi-Sani, L. Lepori, T. Kirova, E. Arimondo, and W. S., arXiv:2507.08439 10.48550/arXiv.2507.08439 (2025).
- [78] K. Black, X. Chen, and T. Byrnes, arXiv:2406.17321 10.48550/arXiv.2406.17321 (2024).
- [79] X. Wang, H. Fan, Z. Bai, and Y. Zhang, arXiv:2504.06678 10.48550/arXiv.2504.06678 (2025).
- [80] F. Cavalcante, Moallison, B. Cakmak, M. V. S. Bonan?a, and S. Deffner, arXiv:2505.20000 10.48550/arXiv.2505.20000 (2025).
- [81] L. Yang, J. Wang, L. Dong, X. Xiu, and Y. Ji, Acta Phys. Sin 74, 100305 (2025).
- [82] T. Wang, Z. Zhang, L. Xiang, Z. Jia, P. Duan, Z. Zong, Z. Sun, Z. Dong, J. Wu, Y. Yin, and G. Guo, Phys. Rev. Appl. 11, 034030 (2019).
- [83] M. D. Lukin, M. Fleischhauer, R. Côté, L. M. Duan, D. Jaksch, J. I. Cirac, and P. Zoller, Phys. Rev. Lett. 87, 037901 (2001).
- [84] R. Han, H. K. Ng, and B.-G. Englert, Europhysics Letters 113, 400001 (2016).
- [85] M. Saffman, J. Phys. B: At. Mol. Phys. 49, 202001 (2016).
- [86] M. Saffman, T. G. Walker, and K. Mølmer, Rev. Mod. Phys. 82, 2313 (2010).
- [87] V. S. Malinovsky and J. L. Krause, Eur. Phys. J. D 14, 147 (2001).
- [88] R. T. Brierley, C. Creatore, P. B. Littlewood, and P. R. Eastham, Phys. Rev. Lett. 109, 043002 (2012).

- [89] K. Bergmann, H. Theuer, and B. Shore, Review of Modern Physics 70, 1003 (1998).
- [90] N. V. Vitanov, A. A. Rangelov, B. W. Shore, and K. Bergmann, Rev. Mod. Phys. 89, 015006 (2017).
- [91] D. Møller, L. B. Madsen, and K. Mølmer, Phys. Rev. Lett. 100, 170504 (2008).
- [92] D. D. B. Rao and K. Mølmer, Phys. Rev. A 89, 030301 (2014).
- [93] I. I. Beterov, M. Saffman, E. A. Yakshina, V. P. Zhukov, D. B. Tretyakov, V. M. Entin, I. I. Ryabtsev, C. W. Mansell, C. MacCormick, S. Bergamini, and M. P. Fedoruk, Phys. Rev. A 88, 010303(R) (2013).
- [94] I. I. Beterov, M. Saffman, E. A. Yakshina, V. P. Zhukov, D. B. Tretyakov, V. M. Entin, I. I. Ryabtsev, C. W. Mansell, C. MacCormick, S. Bergamini, and M. P. Fedoruk, Laser Phys. 24, 074013 (2014).
- [95] K. Tang, Z. Hu, X. Chenand, and C. Liu, Journal of the European Optical Society-Rapid Publications 16, 18
- [96] P. Berman and V. Malinovsky, eds., Principles of Laser Spectroscopy and Quantum Optics (Princeton University Press, 2011).
- [97] F. Petiziol, B. Dive, F. Mintert, and S. Wimberger, Phys. Rev. A 98, 043436 (2018).
- [98] C. A. Sackett, D. Kielpinski, B. E. King, C. Langer, V. Meyer, C. J. Myatt, M. Rowe, Q. A. Turchette, W. M. Itano, D. J. Wineland, and C. Monroe, Nature (London) 404, 256 (2000).
- [99] N. Šibalić, J. D. Pritchard, C. S. Adams, and K. J. Weatherill, Computer Physics Communications 220, 319 (2017).
- [100] K. M. Maller, M. T. Lichtman, T. Xia, Y. Sun, M. J. Piotrowicz, A. W. Carr, L. Isenhower, and M. Saffman, Phys. Rev. A 92, 022336 (2015).
- [101] X. Chen, I. Lizuain, A. Ruschhaupt, D. Guéry-Odelin, and J. G. Muga, Phys. Rev. Lett. 105, 123003 (2010).
- [102] N. Bezuglov, I. Beterov, A. Cinins, K. Miculis, V. Entin, P. Betleni, G. Suliman, V. Gromyko, D. Tretyakov, E. Yakshina, and I. Ryabtsev, arXiv:2411.06607 10.48550/arXiv.2411.06607 (2024).
- [103] I. I. Ryabtsev, I. I. Beterov, D. B. Tretyakov, V. M. Entin, and E. A. Yakshina, Phys. Rev. A 84, 053409 (2011).
- [104] I. Beterov, E. Yakshina, G. Suliman, P. Betleni, A. Prilutskaya, D. Skvortsova, T. Zagirov, D. Tretyakov, V. Entin, N. Bezuglov, and I. Ryabtsev, arXiv:2410.01703 10.48550/arXiv.2410.01703 (2024).